Accepted Manuscript

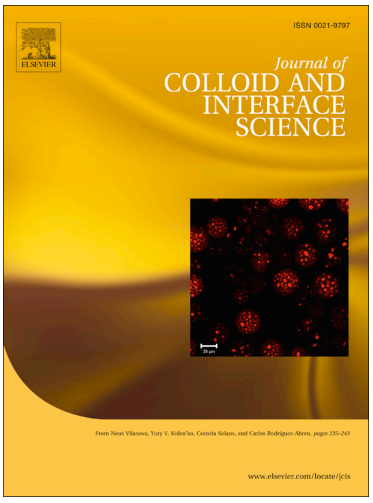

Thin Liquid Film between a Floating Oil Droplet and a Glass Slide Under DC Electric Field

Junyan Zhang, Yongxin Song, Dongqing Li

PII: S0021-9797(18)31105-6
DOI: https://doi.org/10.1016/j.jcis.2018.09.030
Reference: YJCIS 24081

To appear in: *Journal of Colloid and Interface Science*

Received Date: 7 August 2018
Revised Date: 8 September 2018
Accepted Date: 10 September 2018

Please cite this article as: J. Zhang, Y. Song, D. Li, Thin Liquid Film between a Floating Oil Droplet and a Glass Slide Under DC Electric Field, *Journal of Colloid and Interface Science* (2018), doi: https://doi.org/10.1016/j.jcis.2018.09.030

Thin Liquid Film between a Floating Oil Droplet and a Glass Slide Under DC Electric Field

Junyan Zhang[a], Yongxin Song[a] and Dongqing Li[b,*]

[a] Department of Marine Engineering, Dalian Maritime University, Dalian, 116026, China

[b] Department of Mechanical and Mechatronics Engineering, University of Waterloo, Waterloo, ON, N2L 3G1, Canada

*Corresponding author: E-mail: dongqing@uwaterloo.ca

Abstract

Hypothesis

The shape of the liquid film (SLF) between a glass slide and an oil droplet immersed in an aqueous solution is influenced by the direct current (DC) electric field. The liquid film, consisting of the central film region and the meniscus film region, is formed between a floating oil droplet and a glass slide overhead.

Experiments

The SLF was experimentally studied in aqueous solutions of different ionic concentrations and pH values. After the DC electric fields were applied along the glass slide in horizontal direction, the diameter of central film and the thickness of meniscus film were measured by the interference method with an optical microscope.

Findings

The diameter of the central film decreases with the increase in the applied electric fields and declines at higher pH values while increases when the ionic concentration increases. The meniscus film becomes thicker with the increase in applied electric fields and is thicker in pH=11 solution and thinner in pH=3 and 1mM NaCl solution. This is the first study of dynamic thin liquid film under DC electric field, which may be attributed to the balance of dielectrophoretic (DEP) force, colloidal force and the deformable characteristic of the oil droplet.

Keywords: DC electric fields; Oil droplets; Meniscus shape; Liquid film

1. Introduction

Electrokinetic phenomena of a micro-size sphere (soft droplet or rigid particle) near a planar surface are fundamentally important in the fields ranging from colloid surface science [1-3], biochemistry [4-6] to biomedicine [7-9]. It is generally recognized that when a solid surface contacts with an aqueous solution, electrical double layer (EDL) will form on the solid surface in the aqueous solution side. Similarly, the EDL can also be generated when an oil droplet is in contact with an aqueous solution. The electrokinetic phenomena are generated by the interaction of an external electric field and the EDL, such as electroosmotic flow (EOF) and electrophoretic motion. Recently, the electrokinetic motions of small oil droplets and rigid particles near a planar surface are widely investigated by researchers [10-14]. Gao et al [15] numerically studied the effect of a fluid-liquid interface on the electrophoretic motion of a sphere. They found that the electrophoretic velocity of the sphere is enhanced by the fluid-liquid interface and this enhancement will increase with the decrease of the separation distance between the fluid-liquid interface and the sphere. Xuan et al [16] experimentally investigated the electrophoretic motion of a near-wall spherical particle in cylindrical capillaries. They found that the electrophoretic velocity of the same-sized particles is larger in smaller-sized capillaries, which demonstrated the enhanced effect of the near-wall electrophoretic motion. Later in 2015, Liang et al [17] experimentally verified the enhancement of the near-wall electrophoretic motion. More recently, Wang et al [18] developed a three-dimensional model to study the electrokinetic motion of a negatively charged oil droplet that attached to an air-water interface and uncovered the dependence of oil droplet electrokinetic velocity and direction on the magnitude of applied electric fields, zeta potential of the water-air interface and the oil-water interface and the droplet size, etc.

In addition to the studies of the electrokinetic motions of a sphere near a planar surface, considerable investigations were conducted to uncover the interaction forces between a sphere and a planar surface in external electric fields [19-23]. Lee et al [24] numerically and experimentally examined the trajectory of a charged water droplet near an oil-water interface in applied electric fields. They found that when the water droplet is close to an oil-air

interface, the pathway of the water droplet is like a concave parabola, which is probably caused by the distorted electric fields at the oil-water interface. Young et al [25] theoretically investigated the dielectrophoretic (DEP) force and colloidal force on a spherical particle near a nonconducting surface. They found that for the electrophoretic motion of a spherical particle near a planar wall, the small gap between them is determined by DEP force, colloidal force and gravitational force.

It should be realized that the above mentioned studies either focus on the electrokinetic motions of a sphere near a planar surface or the interactions between a sphere and a planar surface. Up to now, there are no theoretical calculations or experimental studies of the thin liquid film formed between an in-water oil droplet and a planar solid surface subjected to an external electric field. However, there were some studies about the measurement of the thin liquid film between a sphere and a planar wall [26-29]. Theodoly et al [30] developed a new model to describe the thin film thickness between a spherical object and a planar surface. Later in 2014, Nikolov et al [31] employed the interference method to study the wetting film stability of a bubble underneath a planar surface. They found that the film thickness, size and the film meniscus could be calculated by the reflected light interferegrams. Captive bubble method is widely used to study the interfacial characteristic [32] and the contact angles [33] formed by a droplet and a flat surface. For example, Baek et al [34] made a comparison of sessile drop and captive bubble method to measure the surface hydrophilicity of a RO membrane, founding that the captive method is reliable and reproducible in measuring the contact angles. Furthermore, Mirchi et al [35] employed the captive bubble method to study the ultra-low dynamic interfacial tension and wettability of shale.

In this paper, the reflected light interference method is applied to examine the effects of DC electric fields on the thickness profile of the liquid film over a floating oil droplet underneath a glass slide. The diameter of the central film and the thickness of the meniscus film were, for the first time, measured under the effect of DC electric fields. The influences of the electric field strength, pH value and the ionic concentration of the bulk liquid on the film thickness profile were discussed. The results in this paper provide a better understanding of the

deformation of a floating oil droplet underneath a glass slide with the effect of applied electric fields.

2. Experiments

2.1. System setup and measurement principle

As shown in Figure 1, the experimental system comprises of a large plastic petri dish (6.4cm in diameter and 2.4cm in height), a small plastic petri dish (5.7cm in diameter and 1.6cm in height), a piece of glass slide (1mm in thickness, 4.9cm in length and 3.9cm in width), an optical microscope (AZ100, Nikon) with a progressive CCD camera (DS-Qi1Mc, Nikon) and imaging software (NIS-Elements BR, Nikon). The small petri dish is placed inside the large petri dish to support a glass slide that is put on top of the small petri dish. A DC power supply (CSI12001X, Circuit Specialist Inc., USA) is used to produce the DC electric field. Two Pt electrodes (with a horizontal separation distance of 3cm) are inserted into a piece of Polydimethylsiloxane (PDMS) that is bonded with the upper surface of the glass slide. The electrodes are then partially immersed into the liquid and connect to the DC power supply with copper wires.

When a micro oil droplet submerged in an aqueous solution is released underneath the glass slide, it will rise up, due the buoyancy, until it reaches the glass slide. Finally the upper surface of the oil droplet slightly deforms and a liquid film is sandwiched between the oil droplet and the glass slide. This liquid film consists of two regions: a central region with a uniform thickness (referred to as the central film) and the rest film with variable thickness in radial direction (referred to as the meniscus film). After applying an electric field parallel to the glass slide, sufficiently large oil droplets will not move in the horizontal direction because strong buoyant force pushes the oil droplet against the glass slide tightly. However, the droplet tends to be deformed in the direction perpendicular to the glass slide under the externally applied electric field. When an external electric field is applied, a strong non-uniform electric field gradient is generated at the small gap region between the oil droplet and the glass slide surface. Consequently an additional repulsive dielectrophoresis

(DEP) force is generated and tends to push the droplet away from the solid surface, leading to a larger thickness of the central film. The diameter of the central film and the thickness of the meniscus film can be measured by the Newton's ring method.

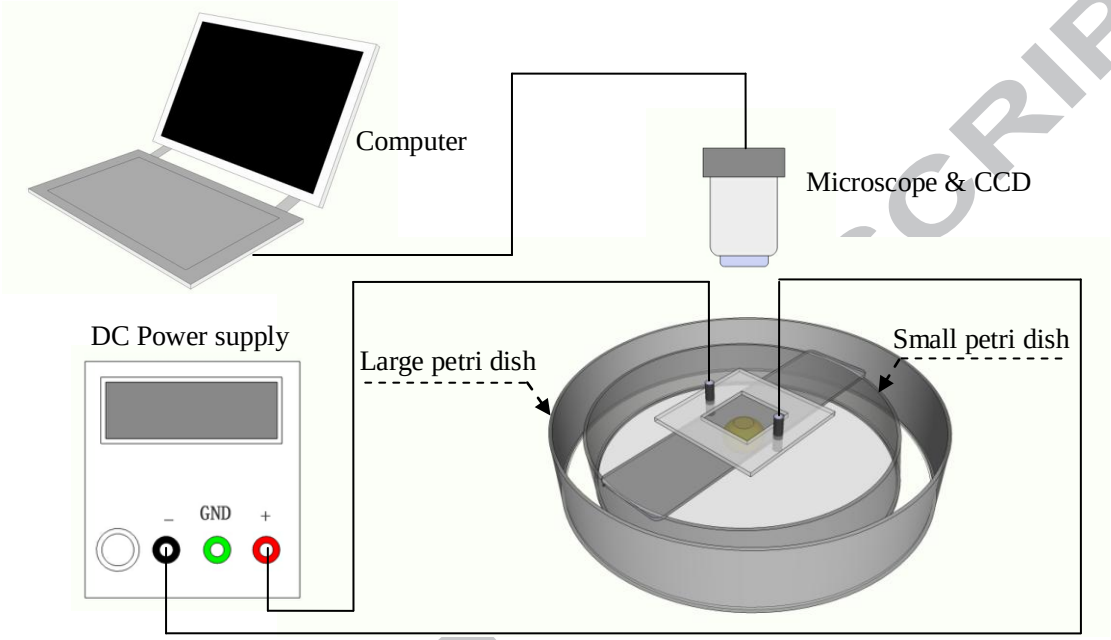

Figure 1. Illustration of the experimental setup.

Figure 2 illustrates the patterns of Newton's rings for the liquid film between the oil droplet and the glass slide. The central dark circle represents the central film region with a diameter D_n. The meniscus film with a variable thickness (h) starts from the edge of the central film to the edge of the droplet. The measuring principle of the liquid film can be simplified as follows: When a parallel beam of monochromatic light is incident normally on the glass slide and the oil droplet, the incident light will be reflected from the surface of the liquid-glass interface and the liquid-oil droplet interface, respectively. As the thickness between glass slide and the oil droplet increases gradually from the origin *o* to the periphery along *x* axis (the radial position discussed below is defined as the distance from the origin *o* along *x* axis.), there will exist optical path difference. According to the optical interference principle, Newton's rings will form when the two beams of the reflected light encounter.

With the measured interference pattern, D_n equals the diameter of the first dark fringe. For the

thickness of the meniscus film, it is given by [36]:

$$h = k\lambda / 4n \quad (k=0,\ 1,\ 2,\ 3,\ 4\ldots) \tag{1}$$

where h represents the thickness of the meniscus film at a bright fringe or a dark fringe position as k is odd or oven, respectively, λ is the wave length of the incident light, n is the refractive index. From Eq. (1), it is easy to find out that the thickness difference between two neighboring fringes is $\lambda/4n$. It can also be noted that for each certain dark or bright fringe, the thickness h is a fixed value. By metering the radial position of each fringe from the origin o and correlate the radial position to the thickness of each fringe, the shape of the meniscus film can be profiled.

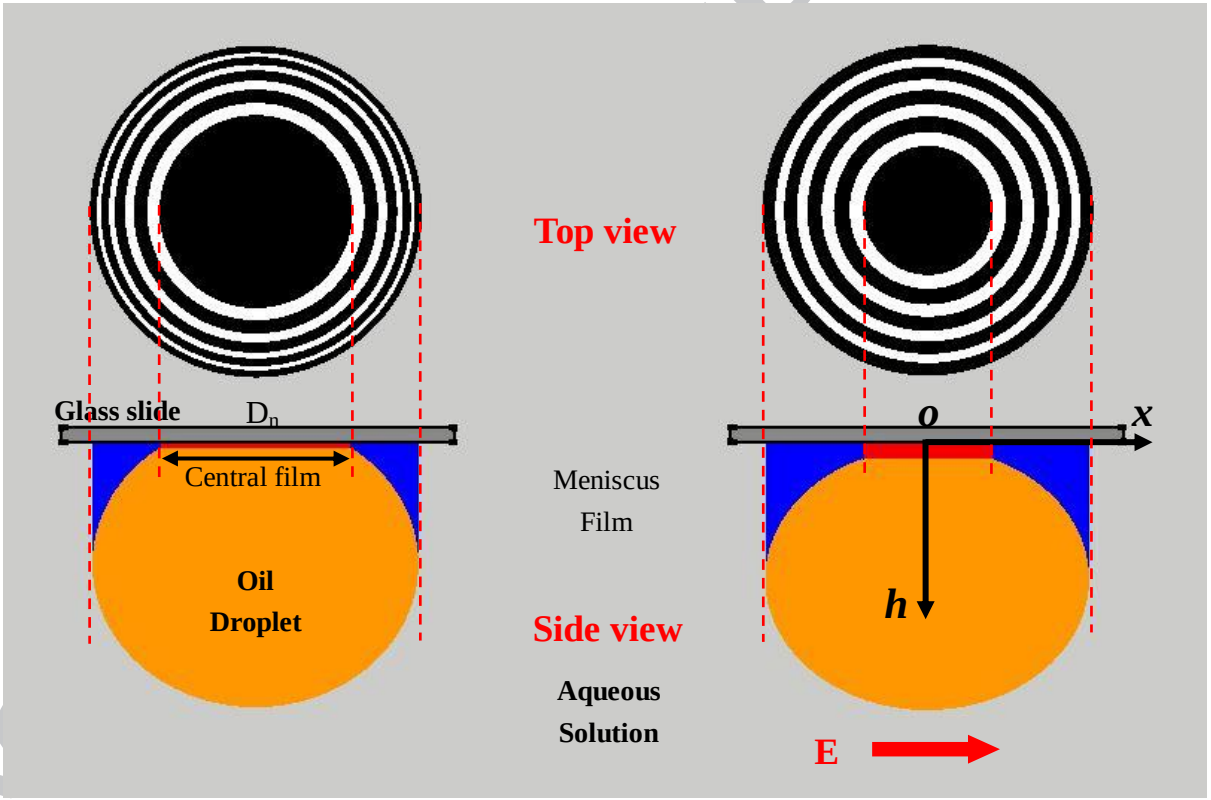

(a) (b)

Figure 2. Illustration of the variations of the central film and the meniscus film, before (a) and after (b) the application of DC electric fields. The central film is the flat pattern area and shown in red color. The meniscus film is illustrated in blue color.

2.2. Materials and experimental procedures

2.2.1. Materials

A vortex mixer (VWR Scientific) was used to emulsify the oil-liquid mixture to obtain micro oil droplets. 50μL silicone oil (0.96g/mL, 50cSt at 25℃, Sigma) was injected into 1000μL aqueous solution and then mixed by the vortex mixer for 10~30s to generate oil droplets in desired microscales. In order to examine the effect of different solutions on the diameter of the central film and the thickness of the meniscus film under the applied electric field, NaCl solutions of 1mM, 0.1mM, and 0.01mM, at pH=3 and pH=11 were used. Each NaCl solution was prepared by the adding certain amounts of NaCl electrolyte into pure water. The pH values were controlled by adding standard solutions of either HCl or NaOH into pure water, respectively.

2.2.2. Experimental procedures

First of all, two petri dishes and a glass slide were cleaned with the testing electrolyte solution and the glass surfaces were purged by pressurized nitrogen gas to remove dust particles. Then, a certain amount of the aqueous solution was added into two petri dishes, so that half of the glass slide was immersed into liquid and the other half was exposed to air. After the system was kept steady for about 5 minutes, oil droplets were released with a 10μL micropipette underneath the glass slide. The oil droplets rose up by buoyance and finally "attached" to the glass slide. Afterwards, two Pt electrodes were inserted into liquid and DC voltages were applied through the DC power supply.

To measure the diameter of the central film region and the thickness profile of the meniscus film by interferograms, a monochromatic light filter (blue light, center wave length is about 440nm) was employed to allow only blue light pass through and reflect on the oil droplets underneath the glass slide. The central fringe diameter and the radial position of each Newton's ring were measured with the imaging system of the microscope. Each data point in all the figures of this paper is the average value of four radial points that uniformly distributed on the circumference of the same Newton's ring. Under each set of conditions, at

least five interferograms were measured. All of the measurements were conducted at room temperature (22±1℃).

3. Theory

For the oil droplet in Figure 2(a), it is subject to a number of forces in the vertical direction, including the buoyant force, the interaction force (in the central film region) between the electric double layer (EDL) of the liquid-oil droplet interface and the electric double layer (EDL) of the liquid-glass interface, and the van der Waals force between the oil droplet and the glass slide. Figure 3(a) depicts the force balance of the oil droplet in *h* axis dirction without the effect of the applied electric field. The thickness of the liquid film at equilibrium state is determined by the force balance in the vertical direction.

$$\vec{F}_{EDL} = \vec{F}_{vdW} + \vec{F}_{b} \tag{2}$$

where F_{EDL} is the EDL interaction force, F_{vdW} is the van der Waals force, and F_b is the buoyance force.

As the oil-liquid interface and the liquid-glass interface are both negative charged, the EDL interaction force is a repulsive force and pointing downwards, which can be expressed by an analytical equation that derived by Hogg et al [37]:

$$F_{EDL} = 2\pi\varepsilon_0\varepsilon a\kappa\left(\zeta_o^2+\zeta_g^2\right)\left[\frac{2\zeta_o\zeta_g}{\zeta_o{}^2+\zeta_g^2}\left(\frac{\exp\left(-\kappa d\right)}{1-\exp\left(-2\kappa d\right)}\right)-\left(\frac{\exp\left(-2\kappa d\right)}{1-\exp\left(-2\kappa d\right)}\right)\right] \tag{3}$$

where ε_0 and ε represent the permittivities of vacuum and the liquid, respectively, ζ_o and ζ_g are the zeta potentials of oil-liquid interface and glass-liquid interface respectively, a is the oil droplet's radius, κ is the Debye-Hückel parameter and κ^{-1} is referred to as the characteristic thickness of the EDL. For the electrolytes with symmetric ions, κ can be expressed as:

$$\kappa = \left(\frac{2e^2z^2n_\infty}{\varepsilon\varepsilon_0k_bT}\right)^{\frac{1}{2}} \tag{4}$$

Where e is the elementary charge, z represents the valence of the ions, n_∞ is the ionic

concentration of the liquid, k_b is the Boltzmann's constant and T is the absolute temperature.

The van der Waals force between the droplet and the flat solid surface is an attractive force pointing upwards and can be expressed [25]:

$$F_{vdW} = \left| \frac{A}{6}\left(\frac{a}{d^2} + \frac{a}{(d+2a)^2} - \frac{2a}{d(d+2a)} \right) \frac{\lambda}{\lambda + sd} + \frac{A}{6}\left(\frac{a}{d} + \frac{a}{d+2a} + \ln\frac{d}{d+2a} \right) \frac{\lambda s}{(\lambda + sd)^2} \right| \quad (5)$$

where λ is the characteristic absorption wavelength and s is a constant; A is the Hamaker constant. For an oil droplet and a solid material interacting in water (w), the Hamaker constant is given by [38]:

$$A = c\left(\sqrt{A_o} - \sqrt{A_w}\right)\left(\sqrt{A_s} - \sqrt{A_w}\right) \quad (6)$$

where A_o, A_s and $A_w = 4.38\times10^{20}$J [38,39] are the Hamaker constants of the oil, solid material and water in vacuum, respectively. The constant c depends on the medium. For water, the constant c is 1.6 [38].

The buoyancy force is the result of the density difference between the oil and the aqueous solution. As the density of the aqueous solution is larger than that of the oil droplet, the buoyancy force is pointing upwards and can be written as [25]:

$$F_b = \frac{4}{3}\pi a^3 g\left(\rho_w - \rho_o\right) \quad (7)$$

where g=9.807 m/s^2 is the gravitational acceleration, ρ_w is the aqueous solution density, and ρ_o is the oil density.

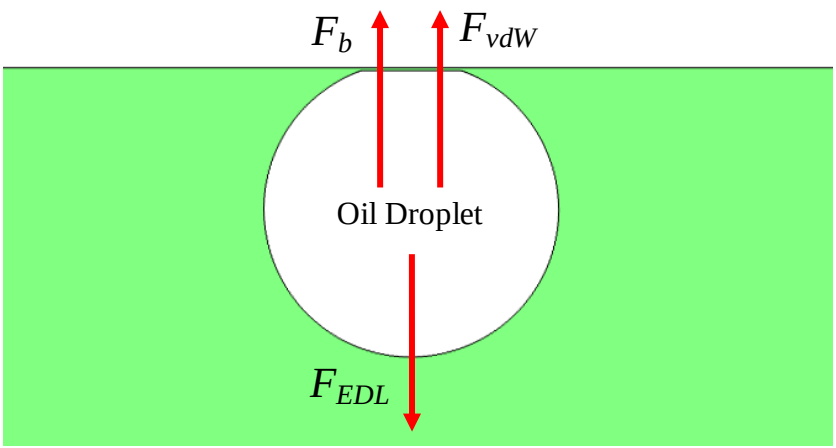

(a)

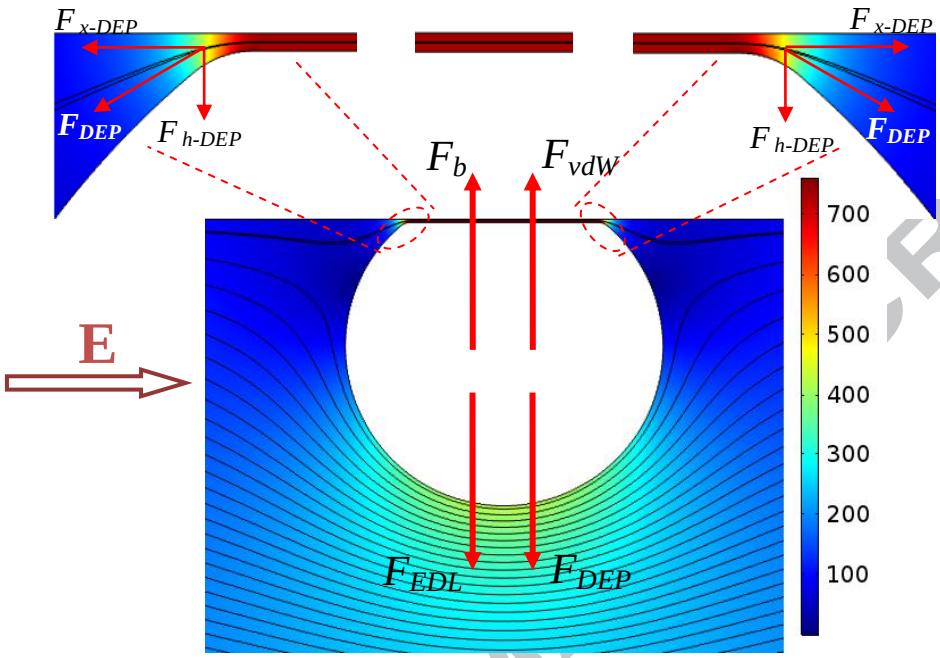

(b)

Figure 3. The force balance in *h* axis on an oil droplet underneath a glass slide before (a) and after (b) applying a DC electric filed in *x* axis, respectively.

After an electric field is applied horizontally, the non-uniform electric field in meniscus film region induces the dielectrophoresis (DEP) force (F_{DEP}). From the gradient of electric field distribution shown in Figure 3(b), it is clear that in the central film region, there exists a strong DEP force acting on the bottom of the oil droplet. Moreover, at the joint of central film region and the meniscus film, the direction of the local DEP forces point to 135° and 225° in Cartesian coordinate system, respectively. If we decompose these DEP forces into *x* axis direction and *h* axis direction, it can be seen that the DEP force in *x* axis direction will be balanced and the net DEP force is in the h axis direction and tends to push the droplet away from the glass slide. The DEP force can be expressed as [40]:

$$F_{DEP} = 2\pi\varepsilon f_{CM} a^3 \nabla |E|^2 \tag{8}$$

where f_{CM} is the Clausius-Mossotti (CM) factor, and E is the strength of the electric field between the oil droplet and the glass slide.

If the oil droplet is under the effect of a DC electric field, then the f_{CM} factor is solely dominated by the conductivity of the oil droplet and the surrounding liquid, as shown in Eq. (9):

$$f_{CM} = \frac{\sigma_o - \sigma_l}{\sigma_o + 2\sigma_l} \quad (9)$$

Where σ_o and σ_l are the electrical conductivities of the oil droplet and the liquid, respectively.

From Eq. (8), it's clear that F_{DEP} is larger under larger electric field. Since the electric conductivity of the aqueous solution is larger than that of the oil droplet, the f_{CM} factor is a negative value. According to Eq. (8), the direction of the DEP force is opposite to the direction of the electric field. Therefore, this DEP force (F_{DEP}) in this system is in the direction from the strong electric field to the weak electric field, that is, from the central film region to the outside. The vertical component of the DEP force (F_{DEP}) will push the oil droplet away from the glass slide. Consequently, the thickness of the liquid film at equilibrium state will be thicker because of the presence of the DEP force or the applied electric field. A larger applied electric field will result in a larger DEP force and therefore the thickness of the central film and the meniscus film will be different under different applied electric fields.

When an external electric field is applied, the thickness of the liquid film at equilibrium state is determined by the following force balance in the vertical direction:

$$\vec{F}_{EDL} + \vec{F}_{DEP} = \vec{F}_{vdW} + \vec{F}_b \quad (10)$$

It should be noted that the the buoyance force do not change with the electric field. The DEP force exerted on the droplet is balanced by the EDL force and the van der Waals force which are all dependent on the separation distance between the glass slide and the oil-liquid interface. Therefore, it can be expected that a change in the separation distance between the oil droplet and the glass slide after applying electric field can be measured and quantified

with the changed Newton's ring pattern.

4. Results and discussion

In order to investigate the liquid film between glass slide and oil droplet, the oil droplet has to be kept immobile in horizontal direction when the electric field is applied along the glass slide. This requires that the oil droplet should be large enough in order to have large buoyancy force to push the oil droplet against the glass slide tightly and thus overcome the drag force exerted by electroosmotic flow. It is found by experiments that the oil droplets that are larger than 200μm in diameter are immobile in horizontal direction under the range of applied electric field used in this study. Therefore, our experimental investigation focuses only on large oil droplets (225μm±5μm in diameter).

4.1. Effects of the applied electric field on the interference patterns

To demonstrate the oil droplet can be deformed by an applied electric field, the interference patterns formed by a floating oil droplet underneath a glass slide under different strengths of electric field were measured and shown in Figure 4. It is obvious that interference rings can be clearly observed. For the measured patterns shown in Figure 4, the diameter of the central film region is equal to the diameter of the central dark fringe. For the meniscus film, the thickness of the meniscus film can be determined by measuring the radial positions of other fringes that are outwards from the central dark fringe. With the increase in the applied electric field, the band width of the outer fringes and the radius of each fringe from the origin *o* become larger. This variation can be observed and quantified by the imaging analysis software.

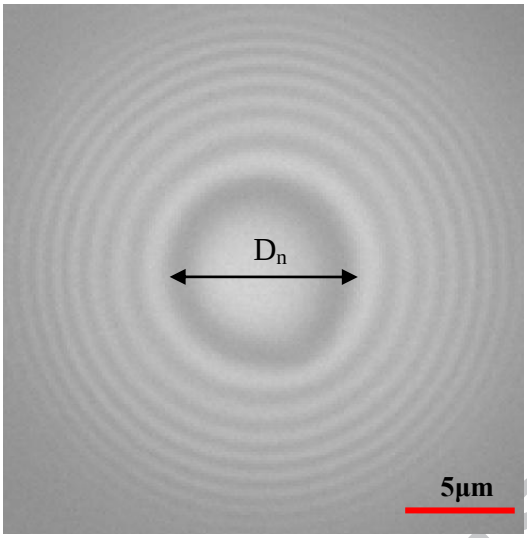

(a)

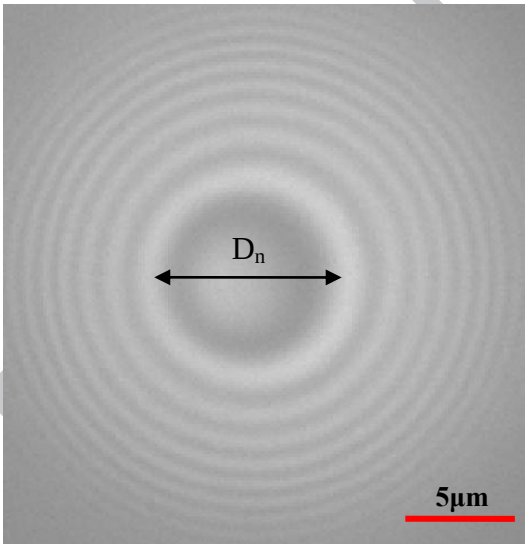

(b)

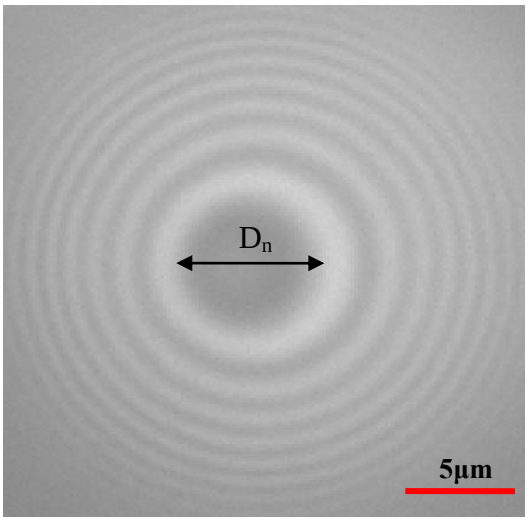

(c)

Figure 4. Evolution of the Newton's rings with applied electric field in pure water. The diameter of the oil droplet is 225μm ± 5μm. The strengths of applied electric field are (a) E=0V/cm, (b) E=30V/cm and (c) E=70V/cm, respectively.

Figure 4 shows the dependence of the diameter of the central film region and the thickness of the meniscus film on radial position. It is clear from Figure 4(a) that when the strength of the applied electric field increases from 0V/cm to 30V/cm, the diameter of the central film region D_n decreases from 8.22μm to 7.91μm. When the strength of the applied electric field increases further to 70V/cm, D_n decreases to 5.54μm. Figure 4(b) shows the dependence of the meniscus film thickness on radial position under applied electric field. As discussed before, the variations of the band width and radius of the fringes under different electric fields, as shown in Figure 4, indicate the change of the thickness of the meniscus film with the applied electric field. From Figure 4(b), it can be seen that for the same radial position, the thickness of the meniscus film is larger when the applied electric field is higher. These relationships can be explained as follows: As the applied electric field influences only on the magnitude of DEP force, from Eq. (8) one can see that when the strength of applied electric field increases, the DEP force increases quadratically. As analyzed above, the DEP force is repulsive and tends to push the oil droplet away from the glass slide. Therefore, it is easy to understand when the strength of applied electric field increases, the contacting region, i.e., the central film region, decreases; and the thickness of the meniscus film increases.

As seen in Figure 5, in comparison with the case of 0V/cm electric field, both of the central film diameter and the meniscus film thickness are almost unchanged in 30V/cm electric field. However, when the strength of the electric field increases to 70V/cm, both of the central film and the meniscus film are changed significantly. This is because under a small strength of applied electric field, the DEP force may not be large enough to overcome the buoyance force and cannot push the oil droplet away from the glass slide. When the strength of the electric field increases further, the DEP force becomes significantly large and is effective to to push the oil droplet away from the glass slide, and hence the diameter of the central film becomes smaller and the thickness of the meniscus film becomes larger.

In this study, we use optical microscope to observe the Newton's interference rings. In the area with Newton's rings, the film thickness changes to form alternative dark and bright fringes. However, the thickness of the central film is uniform in the center film region, resulting in no Newton's rings. Consequently, one cannot measure the thickness of the central film directly by the Newton's ring method. As shown in Figure 2, there is still some distance from the measuring point of the first bright ring to the joint of the central film and the meniscus film. Although the thickness of the central film cannot be directly measured; however, the thickness of the meniscus film at the position of the first bright ring is 0.827μm, the thickness of the central film should be smaller than this value. Furthermore, the thickness of the central film should be a function of the electric field strength; because the DEP force, which is a function of the strength of the electric field, pushes the oil droplet away from the glass slide. The thickness of the central film should also be a function of pH and ionic concentration. The thickness of the central film is determined by the force balance in the vertical direction, i.e., Eq. (2). In the force balance equation, a key component is the F_{EDL} which depends on the zeta potentials of the glass-liquid interface and the oil-liquid interface, and these zeta potentials in turn depend on the pH and the ionic concentration.

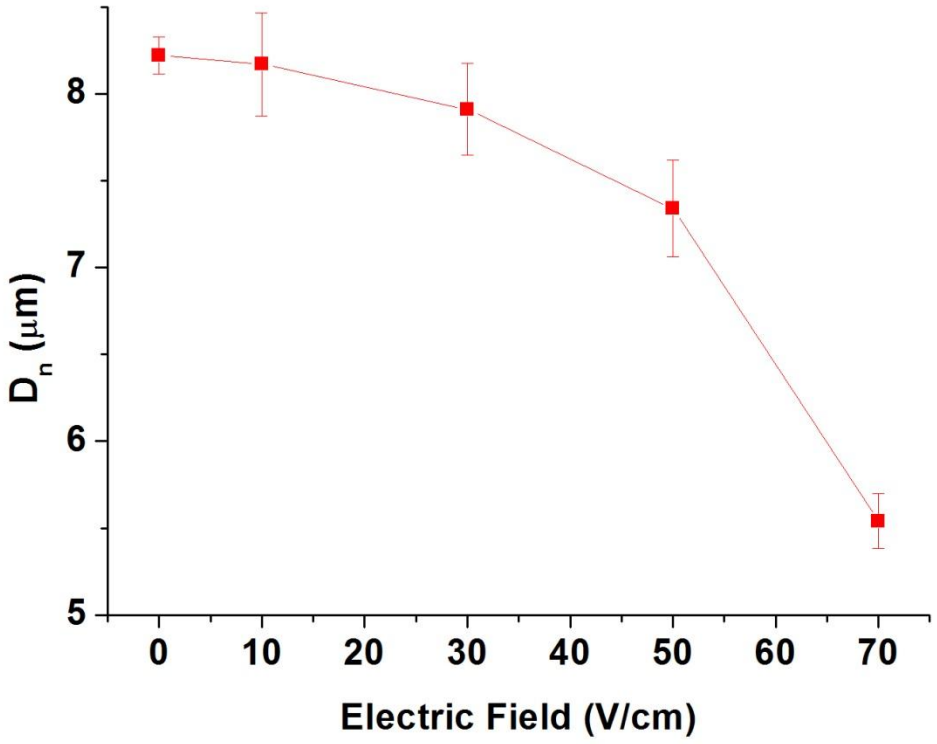

(a)

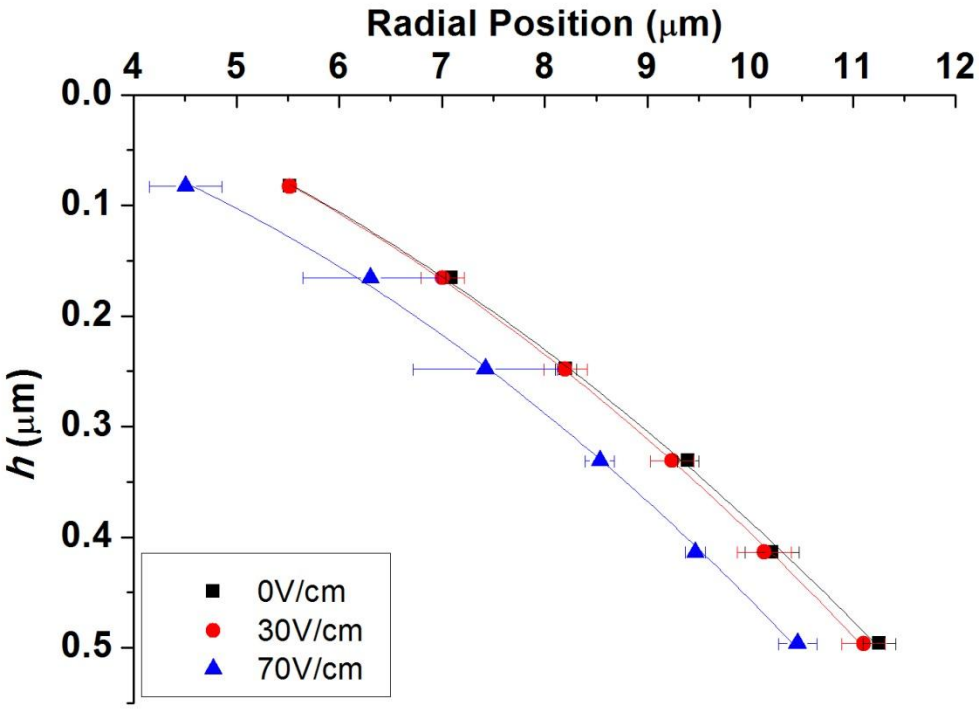

(b)

Figure 5. Evolution of the shape of the liquid film under applied electric field in pure water. The oil droplets have a diameter of 225μm±5μm. (a) Dependence of the diameter of central film region (D_n) on applied electric field. (b) Dependence of the thickness of meniscus film (h) on radial position under different electric fields.

4.2. Effect of pH value on SLF

In addition to the applied electric field, the diameter of the central film and the thickness of the meniscus film are also influenced by the pH values and the ionic concentration of the aqueous solution surrounding the oil droplet and the glass slide. Figure 6 shows the pH dependence of the diameter of the central film and the thickness of the meniscus film under DC electric field. From the inserted table, one can see that for oil droplets under a given electric field, the diameters of the central film are larger in pH=3 solution while are smaller in pH=11 solution. From Figure 6 it can be seen that for the same radial position, the meniscus film thickness is always larger in pH=11 solution while smaller in pH=3 solution.

Such phenomena can be explained by the zeta potential effect. Theoretically, for an immersed oil droplet close to a planar wall, higher zeta potentials in absolute values (both oil-liquid interface and liquid-glass interface) will result in a larger EDL interaction force, as indicated by Eq. (3). The zeta potentials of glass surface ζ_g in pH=11 solution and pH=3 solution are reported to be about –85mV and –43mV, respectively [41] and the zeta potentials of silicone oil-liquid interface ζ_o in pH=11 solution and pH=3 solution are about –55mV and 25mV, respectively [42]. It can be seen from Eq. (3) that when the zeta potentials (both in positive or negative sign) of glass-liquid interface and oil-liquid interface increase, the repulsive EDL interaction force increases dramatically. As the DEP force does not vary with respect to the change of zeta potentials, it is clear that the EDL interaction force is dominant and increases with the increase of pH values. Consequently, the oil droplet is pushed away from the glass slide, resulting in a smaller central film diameter and larger meniscus film thickness. It should also be noted that when pH=3, the zeta potential of the oil droplet-liquid interface is about 25mV. According to Eq. (3), the EDL interaction force turns out to be a negative value, which

means attractive. As a result, the oil droplet is pushed away less and hence the diameter of the central film is reduced less and the thickness of the meniscus film is increased less.

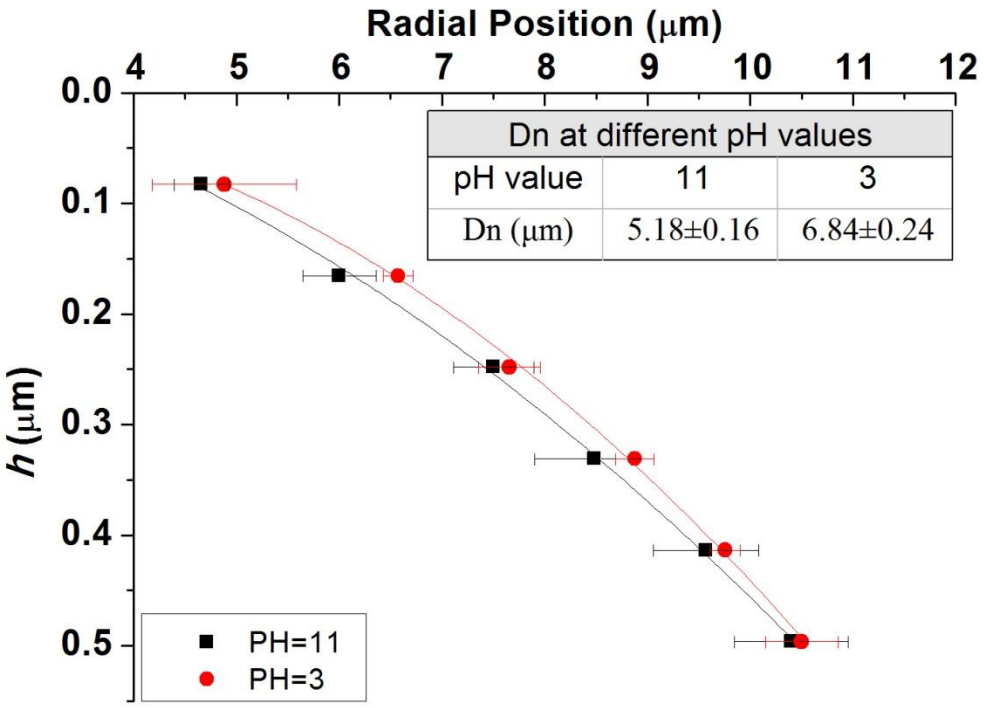

Figure 6. The pH dependence of the meniscus film thickness. The inserted table shows the pH dependence of the central film diameter. The strength of applied electric field is 70V/cm and the oil droplets have a diameter of 225μm±5μm. The liquid is pure water.

4.3. Effect of ionic concentration on SLF

Figure 7 shows the dependence of the diameter of the central film and meniscus film thickness under applied DC electric field on the ionic concentration of NaCl electrolyte solutions. Three concentrations, 0.01mM, 0.1mM and 1mM, were tested in the experiments, respectively. It is clear from the inserted table that, under a given electric field, the diameter of the central film is the smallest in 0.01mM NaCl solution and the diameter of the central film increases with the increase of the ionic concentration of the electrolyte solution. From Figure 7 it can be seen that at the same radial position and under the same strength of electric field, the thickness of the meniscus film is smaller when the ionic concentration is larger.

From Eq. (9) one can see that in DC-DEP system, the f_{CM} factor is determined only by the electrical conductivity of the oil droplet and the electrolyte solution. Compared with the conductivity of the electrolyte solution, the conductivity of oil droplet is infinitely small, or even can be regarded as zero. Therefore, the f_{CM} factor turns to be a constant -1/2 [43]. Therefore the DEP force does not change with the ionic concentration of the liquid in this system. On the other hands, according to Eq. (4), the characteristic thickness of the EDL κ^{-1} decreases dramatically when the ionic concentration of the liquid increases. As a result, the repulsive EDL interaction force between the glass slide and the oil droplet is reduced with the increase of ionic concentration. Apparently, the decrease of the repulsive EDL interaction force with the increase of the ionic concentration is dominant, that is, the oil droplet is pushed away more from the glass slide at lower ionic concentration, resulting in a larger diameter of the central film and a smaller thickness of the meniscus film when the ionic concentration is higher, as shown in Figure 7.

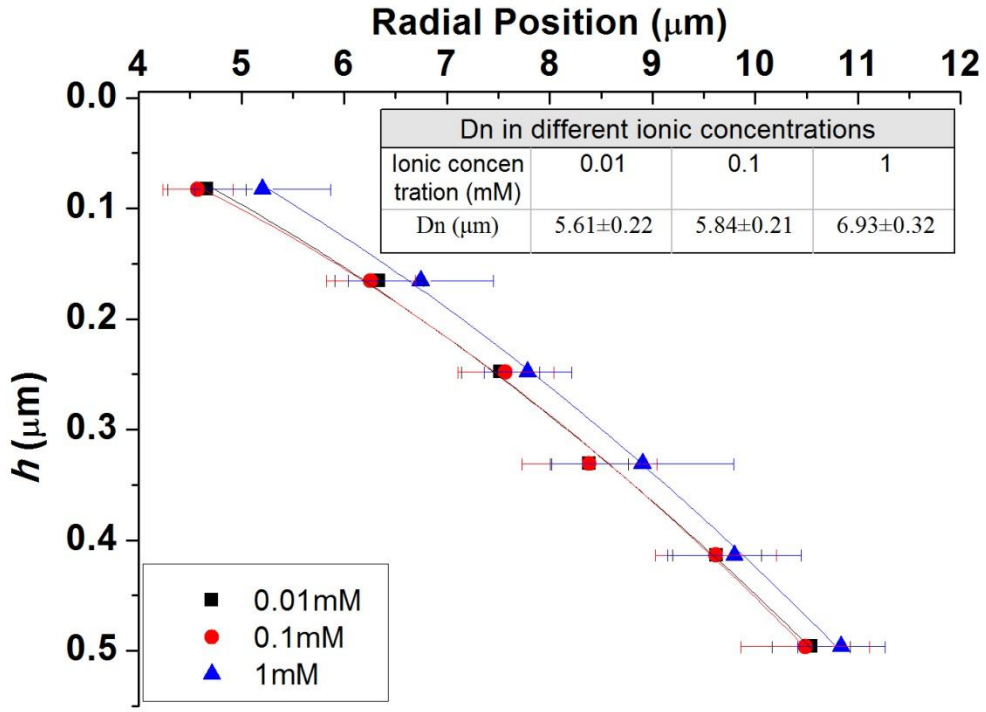

Figure 7. The ionic concentration dependence of the meniscus film thickness. The inserted table shows the ionic concentration dependence of the central film diameter. The strength of applied electric field is

70V/cm and the diameter of the oil droplets is 225μm±5μm.

5. Conclusion

In this paper, the shape of the liquid film over a floating oil droplet underneath a glass slide in applied electric field was investigated for the first time. By using the method of Newton's rings, the diameter of the central film region and the thickness of the meniscus film were measured with an optical microscope imaging system. The experimental results show that with the increase of the strength of the applied DC electric field, the diameter of the central film region decreases. Meanwhile, for the same radial position, the meniscus film thickness under the effect of larger applied electric field strength is bigger than that under the effect of smaller applied electric field strength. Under the same strength of the applied electric field, the diameter of the central film region decreases when the pH increases; and the thickness of the meniscus film is larger at the same radial position in a higher pH solution. The diameter of the central film region is larger and the thickness of the meniscus film is smaller when the ionic concentration of NaCl solution is higher. Compared with the previous studies of thin film measurement by interference method [26-31] and captive bubble method [32-35], this study focuses on the dynamic thin film profiling of an oil droplet below a planar surface under the effect of a DC electric field. This experimental system is capable to dynamically and accurately distinguish tiny variations (In nanometer scale as shown in the figures.) of the thin film profile caused by the electric field. The results from this investigation provide a basic understanding for the future studies on the electrokinetic and electrohydrodynamics phenomena of the thin film formed by a micro droplet underneath a flat surface. Other characteristics of the thin film under the effect of electric field, such as disjoining pressure, will be studied in the near future based on our current experimental method.

Acknowledgement

This work was supported by the National Natural Science Foundation of China to Y. Song [grant number 51679023]; the Fundamental Research Funds for the Central Universities [grant number 3132018261]; and the Natural Sciences and Engineering Research Council of

Canada through a research grant to D. Li [grant number RGPIN-03622].

The authors have declared no conflict of interest.

References

[1] T. Bickel, Hindered mobility of a particle near a soft interface, Phys. Rev. E 75 (2007) 041403.

[2] N. Aubry, P. Singh, Physics underlying controlled self-assembly of micro-and nanoparticles at a two-fluid interface using an E-field, Phys. Rev. E 77 (2008) 056302.

[3] G. M. Wang, R. Prabhakar, E. M. Sevick, Hydrodynamic mobility of an optically trapped colloidal particle near fluid-fluid interfaces, Phys. Rev. Lett. 103 (2009) 248303.

[4] D. Li, Encyclopedia of Microfluidics and Nanofluidics, Springer Science & Business Media, New York, 2008.

[5] R. Westermeier, Electrophoresis in Practice: A Guide to Methods and Applications of DNA and Protein Separations, John Wiley & Sons, New York, 2016.

[6] H. Shintani, J. Polonsky, Handbook of Capillary Electrophoresis Applications, Springer Science & Business Media, New York, 2012.

[7] T. Deisboeck, J. Yasha Kresh, Complex Systems Science in Biomedicine, Springer Science & Business Media, New York, 2007.

[8] D. Li, Electrokinetics in Microfluidics, Elsevier Academic Press, Amsterdam, 2004.

[9] A. P. Lee, L. J. Lee, Biological and Biomedical Nanotechnology, Springer Science & Business Media, New York, 2006.

[10] J. Zhang, Y. Song, D. Li, Electrokinetic motion of a spherical polystyrene particle at a liquid-fluid interface, J. Colloid Interface Sci. 509 (2018) 432-439.

[11] C. Wang, M. Li, Y. Song, X. Pan, D. Li, Electrokinetic motion of a spherical micro particle at an oil-water interface in microchannel, Electrophoresis, 39 (2018) 807-815.

[12] M. S. Kilic, M. Z. Bazant, Induced-charge electrophoresis near a wall, Electrophoresis 32 (2011) 614-628.

[13] J. Bławzdziewicz, M. L. Ekiel-Jeżewska, E. Wajnryb, Motion of a spherical particle near a planar fluid-fluid interface: The effect of surface incompressibility, J. Chem. Phys. 133 (2010) 114702.

[14] L. Liang, Y. Ai, J. Zhu, S. Qian, Xiangchun Xuan, Wall-induced lateral migration in particle

electrophoresis through a rectangular Microchannel, J. Colloid Interface Sci. 347 (2010) 142-146.

[15] Y. Gao, D. Li, Translational motion of a spherical particle near a planar liquid-fluid interface, J. Colloid Interface Sci. 319 (2008) 344-352.

[16] X. Xuan, C. Ye, D. Li, Near-wall electrophoretic motion of spherical particles in cylindrical capillaries, J. Colloid Interface Sci. 289 (2005) 286-290.

[17] Q. Liang, C. Zhao, C. Yang, Enhancement of electrophoretic mobility of microparticles near a solid wall-experimental verification, Electrophoresis 36 (2015) 731-736.

[18] C. Wang, Y. Song, X. Pan, D. Li, Electrokinetic motion of an oil droplet attached to a water-air interface from below, J. PHys. Chem. B 122 (2018) 1736-1746.

[19] M. A. Hamed, E. Yariv, Boundary-induced electrophoresis of uncharged conducting particles: near-contact approximation, Proc. R. Soc. A 465 (2009), 1939-1948.

[20] E. Yariv, H. Brenner, Near-contact electrophoretic motion of a sphere parallel to a planar wall, J. Fluid Mech. 484 (2003) 85-111.

[21] S. Ghosal, The effect of wall interactions in capillary-zone electrophoresis, J. Fluid Mech. 491 (2003) 285-300.

[22] L. Zeng, S. Balachandar, P. Fischer, Wall-induced forces on a rigid sphere at finite Reynolds number, J. Fluid Mech. 536 (2005) 1-25.

[23] S. Kang, Dielectrophoretic motions of a single particle in the vicinity of a planar wall under a direct-current E-field, J. Electrostat. 76 (2015) 159-170.

[24] D. W. Lee, D. J. Im, I. S. Kang, Electrophoretic motion of a charged water droplet near an oil-air interface, Appl. Phys. Lett. 100 (2012) 221602.

[25] E. W. K. Young, D. Li, Dielectrophoretic force on a sphere near a planar boundary, Langmuir 21 (2005) 12037-12046.

[26] L. Limozin, K. Sengupta, Quantitative reflection interference contrast microscopy (RICM) in soft matter and cell adhesion, ChemPhysChem 10 (2009) 2752-2768.

[27] R. C. A. van der Veen, T. Tran, D. Lohse, C. sun, Direct measurements of air layer profiles under impacting droplets using high-speed color interferometry, Phys. Rev. E 85 (2012) 026315.

[28] J. de Ruiter, F. Mugele, D. van der Ende, Air cushioning in droplet impact. I. Dynamics of thin films studied by dual wavelength reflection interference microscopy, Phys. Fluids 27 (2015) 012104.

[29] D. P. Rozairo, A. B. Croll, Late stage drainage of block copolymer stabilized emulsion drops, Soft

Matter, 12 (2016) 9616-9621.

[30] O. Theodoly, Z. H. Huang, M. P. Valignat, New modeling of reflection interference contrast microscopy including polarization and numerical aperture effects: application to nanometric distance measurements and object profile reconstruction, Langmuir 26 (2010) 1940-1948.

[31] A. Nikolov, D. Wasan, Wetting-dewetting films: The role of structural forces, Adv. Colloid Interface Sci. 206 (2014) 207-221.

[32] J. Xue, P. Shi, L. Zhu, J. Ding, Q. Chen, Q. Wang, A modified captive bubble method for determining advancing and receding contact angles, Appl. Surf. Sci. 296 (2014) 133-139.

[33] F. J. Ruiz-Cabello, M. A. Rodriguez-Valverde, A. Marmur, M. A. Cabrerizo-Vilchez, Comparison of sessile drop and captive bubble methods on rough homogeneous surfaces: a numerical study, Langmuir 27 (2011) 9638-9643.

[34] Y. Baek, J. Kang, P. Theato, J. Yoon, Measuring hydrophilicity of RO membranes by contact angles via sessile drop and captive bubble method: A comparative study, Desalination 303 (2012) 23-28.

[35] V. Mirchi, S. Saraji, L. Goual, M. Piri, Dynamic interfacial tension and wettability of shale in the presence of surfactants at reservoir conditions, Fuel 148 (2015) 127-138.

[36] A. Hadjiiski, R. Dimova, N. D. Denkov, I. B. Ivanov, R. Borwankar, Film trapping technique: precise method for three-phase contact angle determination of solid and fluid particles of micrometer size, Langmuir 12 (1996) 6665-6675.

[37] R. Hogg, T. W. Healy, D. W. Fuerste, Mutual coagulation of colloidal dispersions, Trans. Faraday Soc. 62 (1966) 1638-1651.

[38] J. Visser, On Hamaker constants: A comparison between Hamaker constants and Lifshitz-van der Waals constants, Adv. Colloid Interface Sci. 3 (1972) 331-363.

[39] R. Yoon, The role of hydrodynamic and surface forces in bubble-particle interaction, Int. J. Miner. Process. 58 (2000) 129-143.

[40] X. Wang, X.-B. Wang, P. R. C. Gascoyne, General expressions for dielectrophoretic force and electrorotational torque derived using the Maxwell stress tensor method, J. Electrostat. 39 (1997) 277-295.

[41] Y. Gu, D. Li, The ζ-potential of glass surface in contact with aqueous solutions，J. Colloid Interface Sci. 226 (2000) 328-339.

[42] Y. Gu, D. Li, The zeta-potential of silicone oil droplets dispersed in aqueous solutions, J. Colloid

Interface Sci. 206 (1998) 346-349.

[43] B. Cetin, D. Li, Dielectrophoresis in microfluidics technology, Electrophoresis 39 (2011) 2410-2427.